



HAL
open science

Fullerene irradiation leading to track formation enclosing nitrogen bubbles in GaN material

J.G. Mattei, M. Sall, F. Moisy, A. Ribet, E. Balanzat, C. Grygiel, I. Monnet

► **To cite this version:**

J.G. Mattei, M. Sall, F. Moisy, A. Ribet, E. Balanzat, et al.. Fullerene irradiation leading to track formation enclosing nitrogen bubbles in GaN material. *Materialia*, 2021, 15, pp.100987. 10.1016/j.mtla.2020.100987 . hal-03162888v1

HAL Id: hal-03162888

<https://hal.science/hal-03162888v1>

Submitted on 8 Mar 2021 (v1), last revised 2 Apr 2021 (v2)

HAL is a multi-disciplinary open access archive for the deposit and dissemination of scientific research documents, whether they are published or not. The documents may come from teaching and research institutions in France or abroad, or from public or private research centers.

L'archive ouverte pluridisciplinaire **HAL**, est destinée au dépôt et à la diffusion de documents scientifiques de niveau recherche, publiés ou non, émanant des établissements d'enseignement et de recherche français ou étrangers, des laboratoires publics ou privés.

Materialia

Fullerene irradiation leads to track formation enclosing nitrogen bubbles in GaN material

--Manuscript Draft--

Manuscript Number:	MTLA-D-20-00560
Article Type:	Full Length Article
Section/Category:	Opt in to First Look
Keywords:	TEM EELS swift heavy ions GaN nitrogen
Abstract:	<p>Gallium nitride was irradiated with fullerene projectiles having an electronic stopping power above the threshold needed to promote ion track formation. The structural and chemical changes induced by fullerene irradiation were studied through Transmission Electron Microscopy (TEM). High resolution TEM inquiries were performed to identify the structural order along the ion tracks and the strain induced in the lattice neighboring the ion tracks. The TEM investigation pointed out local amorphization inside the whole tracks and High Resolution TEM studies in the track periphery evidence local stress in the wurtzite structure. Chemical investigations were carried out by STEM - Electron Energy Loss Spectroscopy (EELS) to describe the chemical order in the neighboring and inside the ion path. Chemical profiles plotted across ion tracks indicate that the Ga/N stoichiometry is essentially maintained in the core track, an oxidation in the ion track periphery was also detected at the surface. Furthermore, the nitrogen k near-edge fine structure investigation reveals the encapsulation of nitrogen bubbles inside the ion tracks.</p>

Fullerene irradiation leads to track formation enclosing nitrogen bubbles in GaN material

JG Mattei^a, M. Sall^a, F. Moisy^a, A. Ribet^a, E. Balanzat^a, C. Grygiel^a, and I. Monnet^{*a}

^a CIMAP, CEA-CNRS-ENSICAEN-Normandie Université BP5133 F-14070 Caen cedex5 France.

* *Corresponding author:* monnet@ganil.fr

Abstract

Gallium nitride was irradiated with fullerene projectiles having an electronic stopping power above the threshold needed to promote ion track formation. The structural and chemical changes induced by fullerene irradiation were studied through Transmission Electron Microscopy (TEM). High resolution TEM inquiries were performed to identify the structural order along the ion tracks and the strain induced in the lattice neighboring the ion tracks. The TEM investigation pointed out local amorphization inside the whole tracks and High Resolution TEM studies in the track periphery evidence local stress in the wurtzite structure. Chemical investigations were carried out by STEM - Electron Energy Loss Spectroscopy (EELS) to describe the chemical order in the neighboring and inside the ion path. Chemical profiles plotted across ion tracks indicate that the Ga/N stoichiometry is essentially maintained in the core track, an oxidation in the ion track periphery was also detected at the surface. Furthermore, the nitrogen k near-edge fine structure investigation reveals the encapsulation of nitrogen bubbles inside the ion tracks.

KEYWORDS: *swift heavy ions, irradiation, GaN, nitrogen bubbles, transmission electron microscopy, electron energy loss spectroscopy, fine structure*

1. Introduction

Owing to their wide direct band gap, the nitride semiconductors, (Al,Ga,In)N can cover a large spectral range from the near infrared to ultraviolet including the visible region. III-Nitrides exhibit remarkable optical and electronic properties which can provide useful applications such as UV-photodetector, laser diodes and light-emitting diode devices [1-5]. Among these nitride semiconductors, GaN demonstrates a high thermal stability which make this material suitable for use in harsh environment. Therefore, such material intend to become one of the next-generation technologies for space exploration [6,7], where radiation damage can strongly limit the efficiency of these future technologies. The devices will be submitted to particles such as protons, electrons, neutrinos, gamma rays and ions including swift heavy ions. For ions at low energy, the energy loss process will be governed by the nuclear energy losses, S_n . Thus, low energetic ions will generate ballistic collision, either point defects or collision cascades. For such energy, GaN does not behave as a classical semiconductor. In the case of most semiconductors, defects induced by low energetic ions are confined in the material approximately at the implantation distance/depth (projectile range R_p). In GaN, defects accumulation occurs in the projectile range region as well. However, an unusually strong surface peak, attributed to trapping of mobile point defect by the GaN surface, is observed. With increasing fluence, a highly disordered layer (100% of disorder in c-RBS) starts from the surface [8,9]. Some authors claimed that this highly disordered region is in fact nanocrystalline for GaN irradiated with rare earth at high fluencies [10-12] or consist of randomly oriented nanocrystallites and N_2 bubbles interspersed in an amorphous non stoichiometric GaN matrix [13]. In any case, the maximum of damage is reached at the surface and not at the depth where most atomic displacements are induced, near the implantation range. Furthermore, the chemical disorder induced by ion bombardment gives rise to N_2 bubbles formation in the outer layers [13-16].

At higher energy, electronic energy losses, S_e , are predominant and lead to other type of defects: track formation, phase transition and surface nanostructures. Ion track formations are governed by the electronic energy loss process according to various phenomenological models: Coulomb explosion, lattice relaxation and thermal spike [17-21]. High energetic ions, with S_e above 17 keV/nm, usually produce tracks along the ion path in gallium nitride [22]. Undeniably, studies performed on this material have demonstrated that ion bombardment, at normal incidence with a high velocity, leads to discontinuous track formation [23]. In addition, an increase of the electronic stopping power induces latent tracks displaying more continuous morphology/shape [24]. Hu et al. found that swift heavy ion irradiation on GaN produces amorphous tracks and generates lattice stress [25]. The impact produced by the projectile exhibits a circular area i.e. a track containing extended defects such as dislocations [26]. In the surface region, other defects, such as nanoholes, were identified in the case of irradiation at grazing incidence [27]. Recently, A. Kumar et al. have reported that heavy ion irradiation induces the formation of isolated defect clusters which affect electrical properties [28-30]. Therefore, a better understanding of the loss of performance induced by irradiation requires investigating locally at the atomic scale the induced damage.

Transmission electron microscopy (TEM) has been extensively utilized to examine the effect of SHI on GaN materials. In particular, latent tracks were widely investigated to recognize any structural modification. However, very few studies have assessed the chemical order in the ion track region. The main goal of this work was to develop a better understanding of atomic displacement and segregation which take place during (and post) irradiation. Electron energy loss spectroscopy (EELS) allows probing the chemical environment, typically at specific edges of gallium and nitrogen. This way, we were able to investigate, locally, the chemical order in the ion track region.

In a previous study, Sall et al. have reported a phase transition which occurs along the ion path, resulting in an amorphization inside the ion track [31]. Ion tracks were created using fullerene irradiation via two projectiles C₂₀ and C₆₀. Particularly, a full amorphization of the ion tracks originating from C₆₀ were clearly established. However, the structural order inside ion tracks induced by C₂₀ projectiles was not fully understood. Indeed, characterizations were, at this time, performed on a JEOL 2010 microscope and high resolution investigation on ion tracks smaller than 1.6 nm suffered from dynamic and delocalization effects. This new study intends to describe more accurately the structural and the chemical order inside these ion tracks. And to overcome obstacles of previous characterizations, a modern double Cs corrected transmission electron microscope fitted with EELS technique has been used.

2. Experimental details

1. Materials and Methods:

The wurtzite GaN layers used in the current study are 3.5- μm -thick, epitaxially grown on c-plane sapphire substrates by metal organic chemical vapor phase deposition by St Gobain Crystals (Vallauris, France), n-doped ($1.9 \times 10^{18} \text{ cm}^{-3}$).

Samples were pre-thinned prior to irradiation in a plan view configuration. Irradiation on thin sample allows analyzing a region where carbon clusters integrity is conserved, and can still be considered as a single projectile. Samples were prepared by mechanical polishing up to a thickness of 100 μm and then dimpled to a thickness of 10 μm at their centers; followed by argon ion milling (5 keV) using a Gatan precision ion-polishing system. Irradiations were carried out at RT under normal incidence using 40 MeV C₆₀ fullerene beams provided by the tandem accelerator at the Institut de Physique Nucléaire d'Orsay, IPNO, (Orsay, France). The 40 MeV C₆₀ ion beam was, to a certain degree, contaminated by 12 MeV C₂₀. It should be noted that the implantation region of the ions is avoided and the slowing down regime is predominately ruled by electronic processes.

For each irradiation, Table I displays the corresponding S_e, the energy deposited by electronic excitation for a given fluence.

Projectile	Energy (MeV)	Se (keV.nm ⁻¹)	Fluence (ions.cm ⁻²)
C ₆₀	40	59	1E ⁺¹¹
C ₂₀	12	19	1E ⁺¹¹

Table 1 - Irradiation parameters for C₆₀ and C₂₀ projectiles in GaN. Se value corresponds to the value at the entrance in the target

2. Characterization techniques:

High resolution TEM and STEM experiments were performed on a double corrected JEOL ARM 200F operating at 200 kV fitted with a GIF Quantum Gatan energy filter. In STEM mode, this microscope provides a spatial resolution of 0.078 nm. STEM analyses were carried out using an HAADF detector at inner and outer angles of 68 and 280 mrad to efficiently reduce diffraction contrast. EELS experiments were performed with a collection angle of 90 mrad. Elemental mapping were recorded with a dispersion

of 1eV/channel while ELNES spectra were acquired using an energy dispersion of 0.025eV/channel providing an energy resolution of 0.5 eV. HR-TEM/STEM micrographs and EELS data were acquired and processed under Gatan Digital Micrograph environment.

3. Results/discussion

We investigated a gallium nitride sample irradiated with fullerenes. For this study, two kinds of projectiles were used: 40 MeV C₆₀ and 12 MeV C₂₀ which provides respectively a Se of 59 and 19 keV/nm (table 1). Such electronic stopping powers are sufficient to overcome the Se threshold (17 keV/nm) in gallium nitride and consequently, to promote ion track formation.

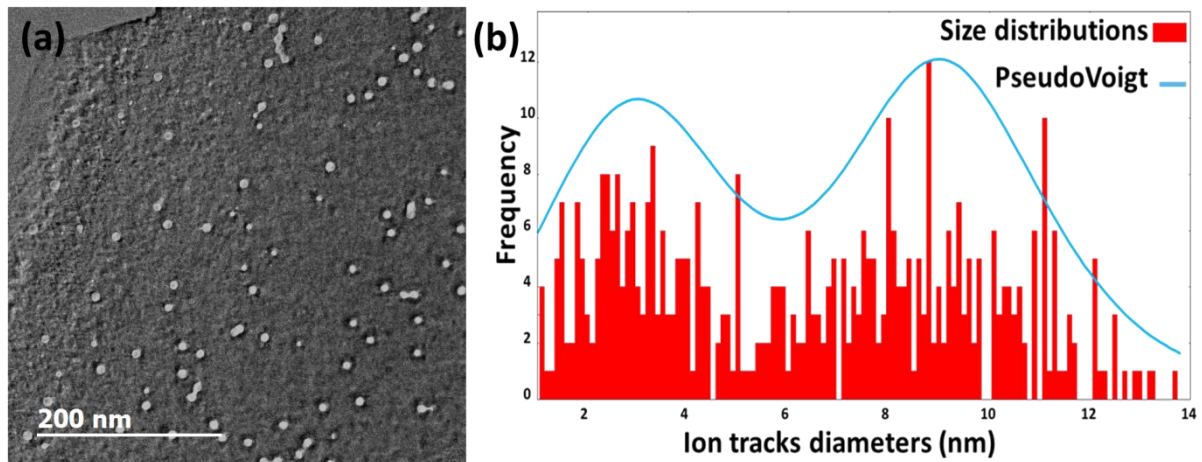


Fig. 1. a) TEM plan view micrograph of GaN irradiated, b) Size distribution of ion tracks diameters.

TEM investigations revealed different latent tracks induced by fullerene projectiles. The TEM micrograph of a GaN specimen plan view, displayed in Fig. 1a, shows several tracks diameters. Most of the tracks are isolated but we can still observe some overlapping tracks. A size distribution was performed on 427 ion tracks to get a better statistic. Size distribution (Fig. 1b) reveals two kinds of populations. This size fluctuation may depend on the target thickness, or ion track overlapping. A first ion track population, assigned to C₂₀ projectiles, displays a mean diameter of 2.8 nm. The second population, originating from C₆₀ projectiles, exhibits a higher mean diameter of 8.5 nm.

Latent tracks observed on Fig. 1 display a brighter contrast compared to their surrounding region, this could be attributed to the loss of matter in the track region and/or to structural modification. Thus, high resolution TEM investigations were carried out to describe the structural order within ion track region.

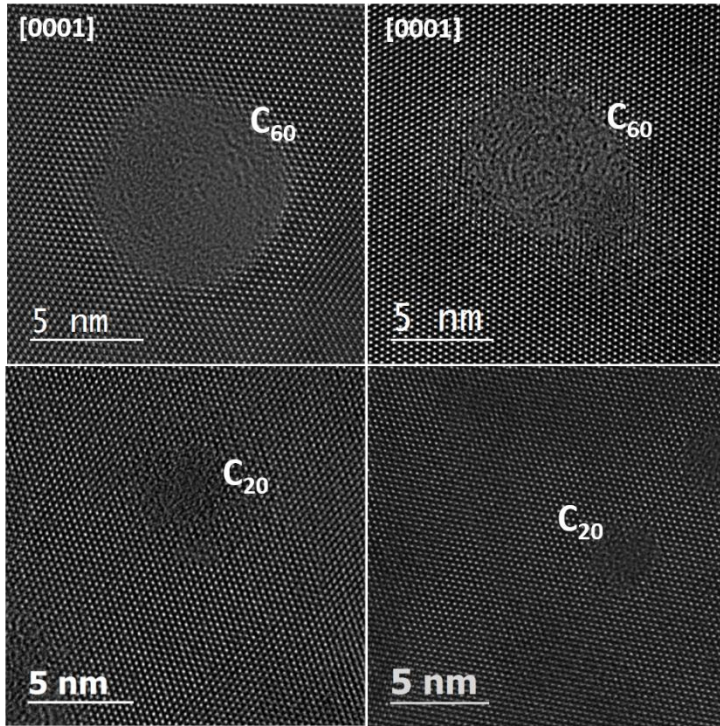


Fig. 2. High-Resolution TEM micrographs of amorphous ion tracks. Plan views of wurtzite GaN are oriented along the [0001] zone axis.

High resolution TEM analyses were performed along the [0001] zone axis of the wurtzite structure. TEM images (Fig. 2) exhibits two types of track diameters: larger tracks correspond to C₆₀ projectiles while smaller tracks are assigned to C₂₀ projectiles. High resolution TEM investigations of the structural modification induced by SHI give evidence of an amorphization localized in the whole track whatever the projectile is (C₆₀ and C₂₀). This is a new result compared with the last study which clearly establishes irradiation with C₂₀ leads to amorphous track as well [31]. It should be noted that during TEM investigations, electron beam could induce a partial recrystallization of the ion track.

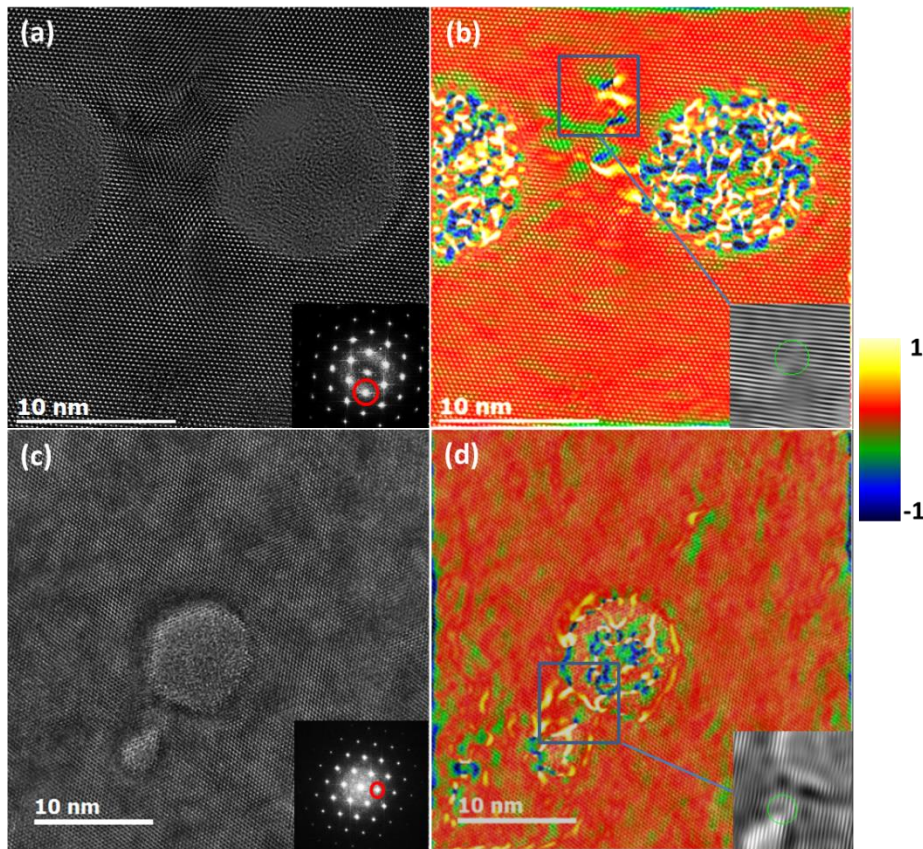


Fig. 3. a) HRTEM image of GaN plan view along the [0001] zone axis, the FFT is displayed in an inset, b) micrograph superimposed to the strain map of $(0\bar{1}10)$ reflexion measured by geometrical phase analysis (zoom of a dislocation is shown in the inset), c) HRTEM micrograph of C_{60} and C_{20} projectile and its respective, d) GPA strain map of $(10\bar{1}0)$ (zoom of dislocation is shown in inset).

In addition, the investigation of the structural order on the track borders revealed some defects induced by ion bombardments. This stress seems to occur along the $(0\bar{1}10)$ planes. Fig. 3a shows a high resolution TEM micrograph oriented along the [0001] zone axis of the wurzite structure. Two ion tracks originating from two C_{60} projectiles are observed in this image, between these tracks clear defects are identified. To illustrate this result, Geometric Phase Analysis was performed to map the displacement of the planes associated to the $(0\bar{1}10)$ reflexion. The colored map superimposed to the HRTEM micrographs shows the variation $(\delta[0\bar{1}10])$ of the lattice plane spacing (Fig. 3b,d). Thus, this displacement map reveals clear defects between tracks such as dislocations (Fig. 3b). Some stress was recognized on the track border as well. Thus, Fig. 3c displays a TEM micrograph in which we can observe two ions tracks. The small one is related to a C_{20} projectile, and conversely larger track has been generated by a C_{60} projectile. An extended defect is identified in between these two tracks. The strain mapping (deriving from GPA analysis) focused on this reflexion demonstrated a clear default in between these two ion tracks generated by C_{20} and C_{60} (Fig. 3d), such as a stacking fault or a misfit dislocation. Furthermore, this strain map reveals some strain localized around the ion track periphery of C_{60} projectiles. This strain is not localized exactly on the track border but about 1.5 nm around the ion track. Strain identified around the track could be related to a defect induced by the ion track or linked to nanohillock formation in surface, resulting in a surface thickness alteration surrounding the ion track.

Further, we carried out scanning transmission electron microscopy in high-angle annular dark-field (HAADF) mode to check the intensity in the ion track periphery. Fig. 4 shows a STEM HAADF image containing several ion tracks. On the track border, an increase of the intensity is clearly observed if we compare to the bulk intensity. As HAADF intensity is proportional to the square of the atomic number, $I_{\text{haadf}} \sim t.Z^2$. This result could be related to a higher density of both gallium and nitrogen. However, t parameter is assigned as the thickness of the sample. Thus, this higher intensity could be linked to an increase of the thickness surrounding the ion track. Moreover, it has been also reported that higher HAADF intensity could be related to strain field as well [32]. To find answer to these questions, we investigated the chemical order in the neighbourhood of an ion track to identify any change in the nitrogen or gallium track content.

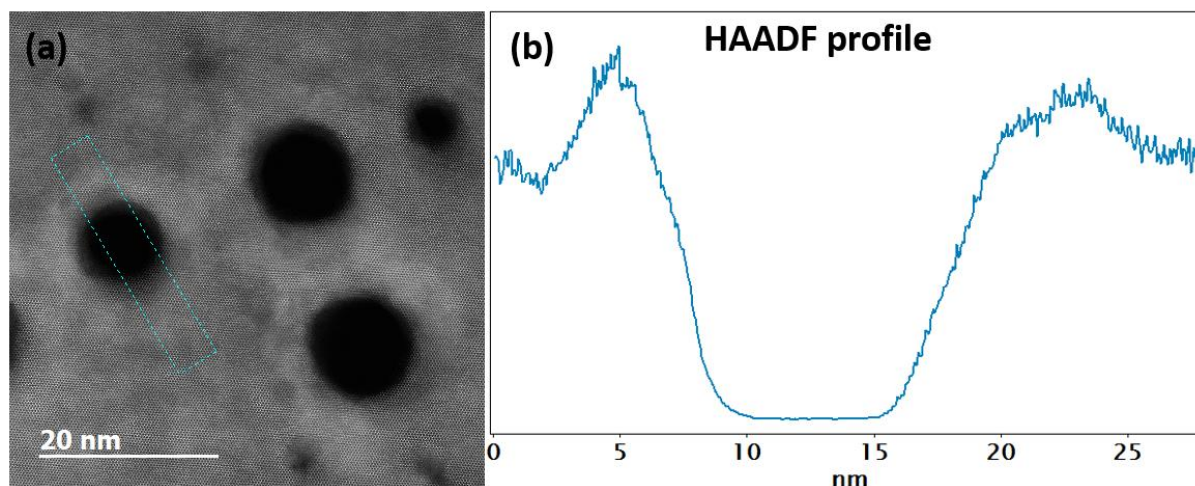


Fig. 4. a) A plan view HAADF image of GaN exhibiting latent tracks, b) HAADF intensity profile of a latent track

Thus, EELS analyses were carried out at different ionization edges: nitrogen K edge and gallium L_{2,3} edge. Furthermore, this technique is quite sensitive to light element such as carbon or oxygen, for that reason we focused as well on the oxygen K edge. Hence, we performed an EELS mapping on a specific ion track induced by C₆₀ (Fig. 5a). EELS mapping at gallium and nitrogen edges confirm a decrease, into the track of their respective ratio to the bulk concentration. The relative decrease of Ga and N is basically the same, indicating that stoichiometry is preserved. Besides, oxygen K edge were also observed on EELS spectra and localized exactly on the track periphery. This result is all the more enhanced on the EELS profile, originated from EELS mapping and plotted along a line crossing the whole ion track diameter (Fig. 5b). As such, we can observe a clear enhancement of the oxygen ratio on the track border. We must recall here that STEM analyses are 2D projections. Hence, we cannot affirm if oxidation occurs on the surface or inside the material. Besides, irradiations were performed at normal incidence, directly on a GaN plan view TEM sample, and SHI are well known to induce nano hillocks at the surface. It is most likely that oxygen is adsorbed in the periphery of such hillocks as we did not find any TEM evidence of the formation of known oxides phases.

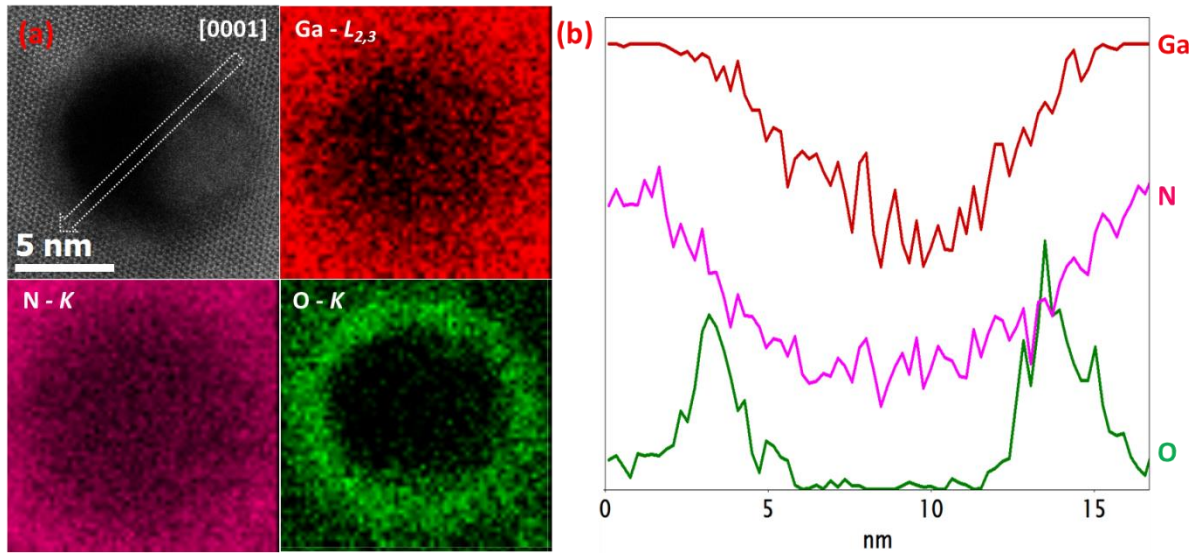


Fig. 5. a) HAADF image and EELS mapping of gallium $L_{2,3}$ edge (red), nitrogen K edge (purple) and oxygen K edge (green), b) EELS profile of Ga, N and O across ion track

To go further and to describe the local atomic environment in the track region, we investigated the Energy Loss Near Edge Structure (ELNES) at nitrogen K edge. Indeed, many studies have been performed at nitrogen edge for this kind of material. Nitrogen edge fine structure could be useful to distinguish hexagonal to a cubic phase in gallium nitride for instance. Thus, fine structure studies were first performed using point EELS analysis in three different regions: bulk region, track border and the track core region (Fig. 6a). Fig. 6b shows the different ELNES spectra acquired in these 3 regions. Nitrogen K edge fine structure in the bulk region (spectrum 1) displays a specific shape of the hexagonal wurzite gallium nitride (h-GaN) [33], however EELS analysis in the track border shows a pre-peak (ELNES spectrum 2), finally nitrogen K edge fine structure inside the ion track shows a thinner peak at 398 eV (ELNES spectrum3).

Two dashed arrows are displayed to illustrate peaks composing the near edge fine structure (A and B). From our experimental data ΔAB is about 2.4 eV which is consistent with Lazar observation for h-GaN [33]. Moreover, we can clearly observe an enhancement of A-peak intensity related to the track border region. Katsikini et al. have observed this type of fine structure using XANES investigations [34]. According to the literature, point defects usually lead to empty states in the midgap depending on different configurations: nitrogen interstitial, substitution of Ga with N atom (N_{Ga}) and substitution of N with Ga atoms (Ga_N). They first excluded substitution of N atom with Ga; consequently such atomic arrangement would lead to Ga-Ga bonds which could not be identified at nitrogen K edge. Nitrogen interstitial signature is supposed to be localized 1.7 eV below the N K edge which is not clearly observed on Fig. 6. According to their study, A-peak could be related to nitrogen dangling bonds which means that gallium atom is missing. Finally, A-peak could be assigned as a gallium vacancy; moreover this result is also supported by the work of Xin [35]. Their study at N K ELNES performed by EELS analyses evidence a pre edge similar to A-peak. This peak was identified on a pure edge dislocation with a Ga vacancy.

However, the nitrogen K edge ELNES 3 displays a thinner single-peak with a higher intensity which is quite different from that of the h-GaN fine structure. Indeed, many studies have reported such fine structure for nitrogen gas; Lacroix et al. evidenced molecular N_2 inside nanopores in a SiO_xN_y matrix,

the ELNES spectrum of N₂ fine structure reported in this paper is clearly comparable to our result [36]. Kovacs et al. identified a similar fine structure by recording EELS spectrum in TEM under molecular gas N₂ environment [37]. These experiments were performed to prove the inclusion of N₂ molecules in a GaN matrix. Indeed, the nitrogen Kedge ELNES observed on the spectrum 3 is the specific signature of N₂ molecule. Thus, this result evidences the presence of dinitrogen gas inside the ion track. Furthermore, we should remind this TEM plan view was prepared by ion milling with 5keV Ar⁺ and then exposed to fullerene bombardment. Thus, low energetic ions which could be provided by Focus Ion Beam and thus inducing point defect were avoided. Therefore, dinitrogen gas formation is clearly related to C₆₀ impacts.

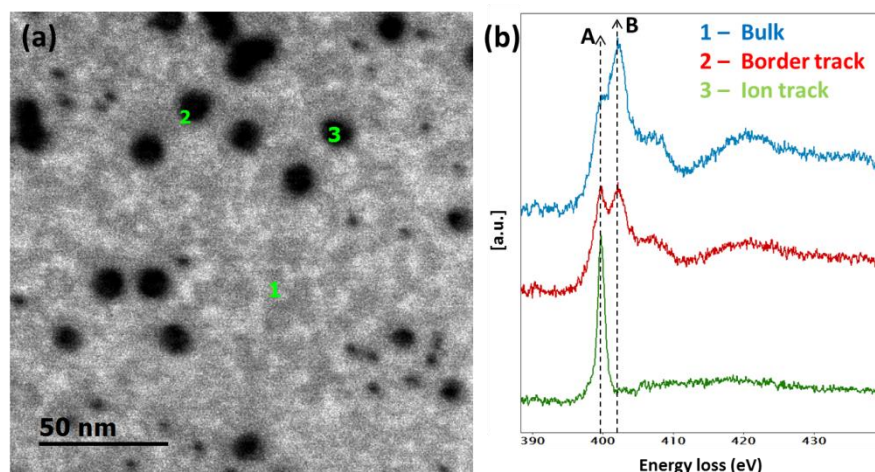


Fig. 6. a) A plan view HAADF image of GaN and latent tracks b) Nitrogen K – ELNES spectra in several regions: 1-bulk region in blue line, 2- track border (spectrum plotted in red), 3- ion track core (green spectrum).

Concerning the ELNES observed on the track border (spectrum 2 - red spectrum), another explanation would be that enhancement of A-peak is explained by a superposition of N₂ and h-GaN fine structure [37]. However, we observed such overlapping in our experiment; A-peak appears to be more intense than B peak related to h-GaN. Therefore, A peak in the ELNES spectrum 2 could be likely attributed to Ga vacancy, in agreement with the study of Xin et al. [35].

To go further, we performed EELS mapping on several tracks in order to increase the statistic. EELS spectra were acquired with an energy resolution of 0.025eV/channel in order to map the nitrogen K edge fine structure (Fig. 7). Defining the spatial distribution of chemical states requires distinguishing h-GaN fine structure from N₂ fine structure. Thus, we performed, using digital micrograph software, Multiple Linear Least Squares (MLLS) fitting according to two near edge fine structures references: N₂ gas and h-GaN. MLLS fitting enables to differentiate these two environments and to fit these specific fine structures in the spectrum image.

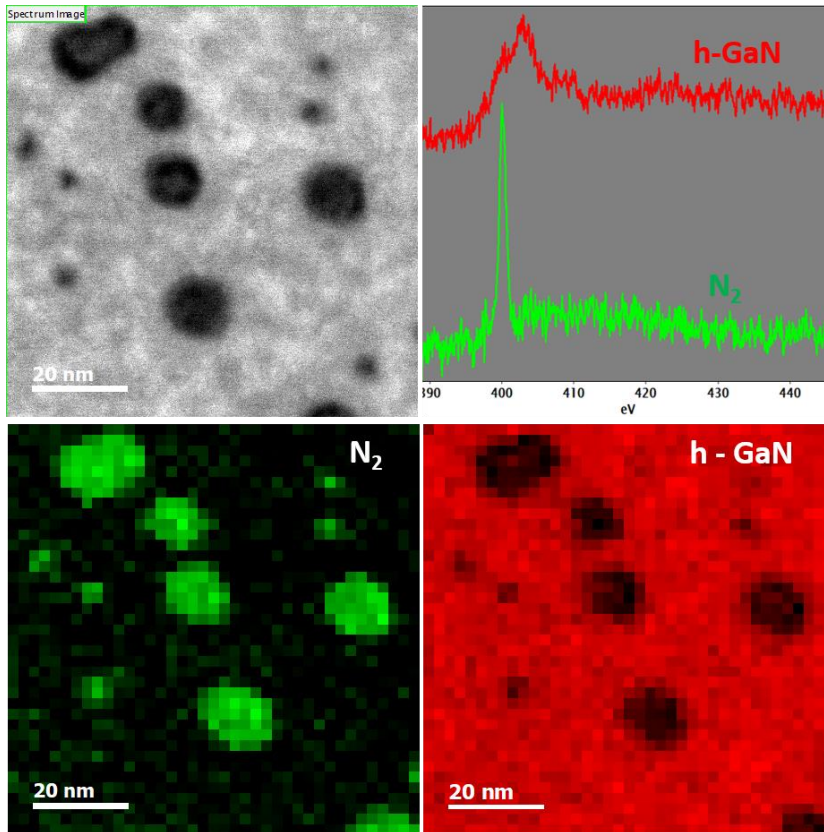


Fig. 7 a) STEM HAADF image b) h-GaN and N₂ reference spectra c) Nitrogen K near-edge structure mapping for N₂ (green) d) ELNES for h-GaN (red)

Fig. 7a shows the HAADF image probed for EELS analysis, the two ELNES references for N₂ molecule and for the hexagonal GaN (h-GaN) (Fig.7b) and the respective ELNES mapping (Figs.7 c and d). Thus, ELNES mapping revealed h-GaN is mainly localized in the bulk part as expected. ELNES h-GaN intensity is quite low in the track region due to the amorphization of GaN. On the contrary, nitrogen fine structure specific of nitrogen gas was observed inside each ion track. Thus, this result clearly evidences N₂ gas is trapped within every ion track. Thus, dinitrogen gas formation is clearly related to C₆₀ and to C₂₀ impacts as well.

Several previous studies have also reported the formation of nitrogen bubbles in a GaN matrix submitted to irradiation. However, these irradiations were performed in the nuclear energy losses range (1 or 2 MeV Au+), which induce point defects, leading to amorphization of GaN in surface. Kucheyev et al. reported that N₂ formation induces a high nitrogen loss in GaN matrix [9]. In our case, fullerene irradiation produces, locally, a high intense electronic excitation which induces a confined enhancement of the temperature. According to gallium nitride phase diagram, a temperature beyond 1117 K decomposes GaN into pure gallium liquid and nitrogen gas [38,39]. Consequently, as nitrogen gas was identified in this ion track, this suggests a pure gallium formation as well, which would be consistent with the in-track conservation of the bulk Ga/N stoichiometry observed in Fig. 5b.

Nevertheless, it should be noted that some authors identified N₂ bubbles formations in an amorphous layer of GaN induced by irradiation at lower energy (4.7 MeV Au), however no Ga-Ga bonding were identified. Indeed, they observed a great decrease of Ga coordination number [13]. Other reports pointed out that, in addition of N-N bonds, Ga-Ga bonds were created as well by phase segregation during

1 irradiation and that nitrogen bubbles induce, locally, high pressure on the lattice [14,40,41]. Apart from
2 the controversy about Ga-Ga bonds, this observation is consistent with the extended defects identified
3 in the ion track periphery in our high resolution TEM investigations. Accordingly, the stress identified
4 on the track region could be related to a high-pressure induced by nitrogen bubbles.
5
6
7
8

9 **4. Conclusion**

10 Gallium nitrides were irradiated with C₂₀ and C₆₀ clusters using a Se above the electronic stopping power
11 threshold, efficient to induce ion track formation. Despite the cluster size, both projectile lead to phase
12 transition. TEM investigation pointed out local amorphization inside the whole tracks and High
13 Resolution TEM studies in the track periphery evidence local stress in the wurtzite structure. EELS
14 analyses demonstrated chemical environment changes such as oxidation in the track border, while a
15 reduction of nitrogen and gallium content was identified inside tracks. The analysis of nitrogen K edge
16 fine structure revealed a fine structure typical of gallium vacancy in the track periphery while a clear
17 signature of dinitrogen gas fine structure was observed inside the track. This specific signature of N₂
18 was observed in each ion track, which gives evidence of encapsulation of nitrogen bubbles inside the
19 ion tracks. To the best of our knowledge, this is the first time nitrogen gas, or nitrogen dimmer is
20 observed specifically inside ion tracks produced by SHI.
21
22
23
24
25
26
27
28
29
30
31
32
33
34
35
36
37
38

39 **Acknowledgements**

40 The authors would like to thank the ALTO accelerators team for providing the ion beams. M. Sall. is
41 grateful to the “Région Basse-Normandie” for its partial contribution to his doctoral grant. This work
42 was partially supported by the ANR funding “Investissements d’avenir” ANR-11-EQPX-0020 (Equipex
43 GENESIS) and ANR-10-LABX-09-01 (LabEx EMC3), by the “Fonds Européen de Développement
44 Regional” and by the Region Basse-Normandie.
45
46
47
48
49
50
51
52
53
54

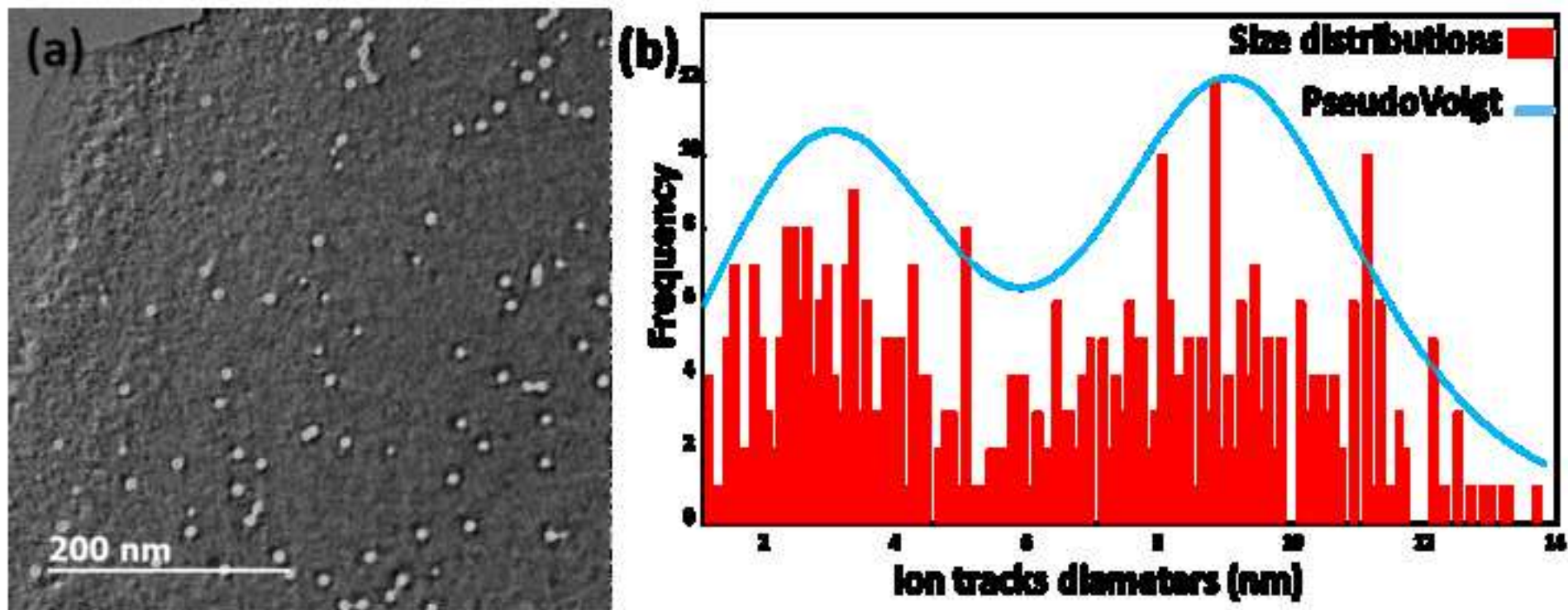
55 **Additional Information**

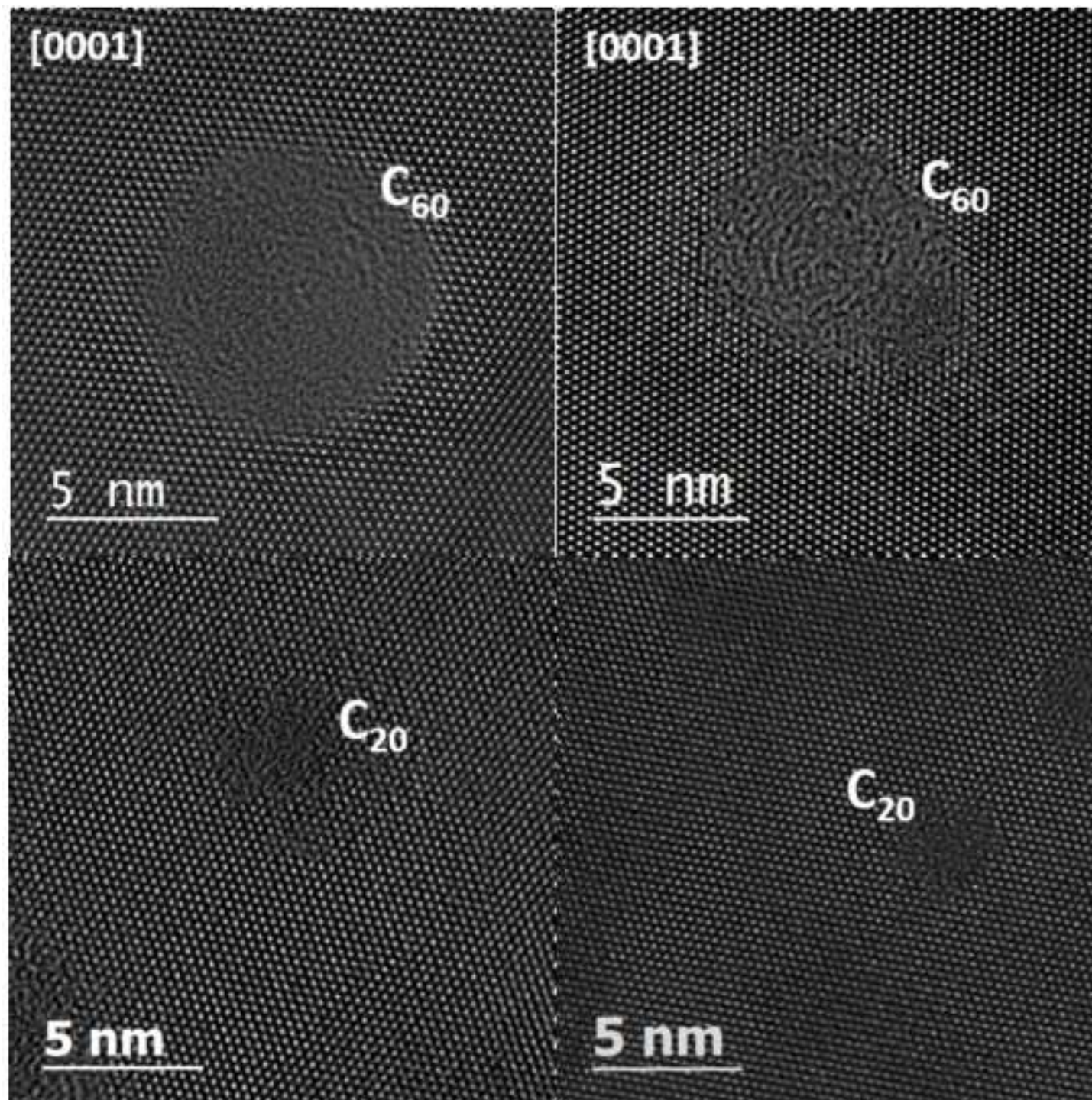
56 Competing Interests: The authors declare no competing interests.
57
58
59
60
61
62
63
64
65

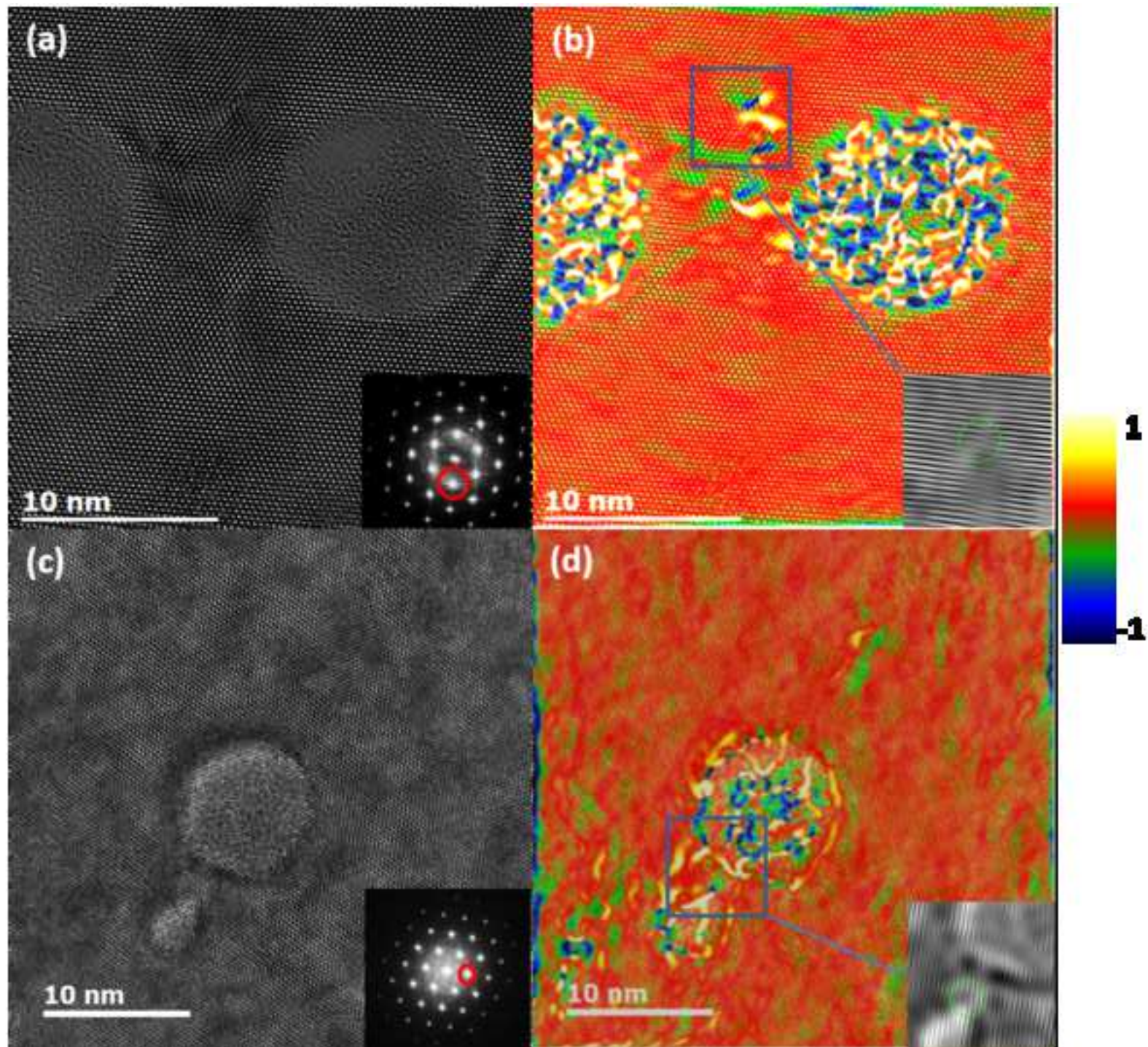
References

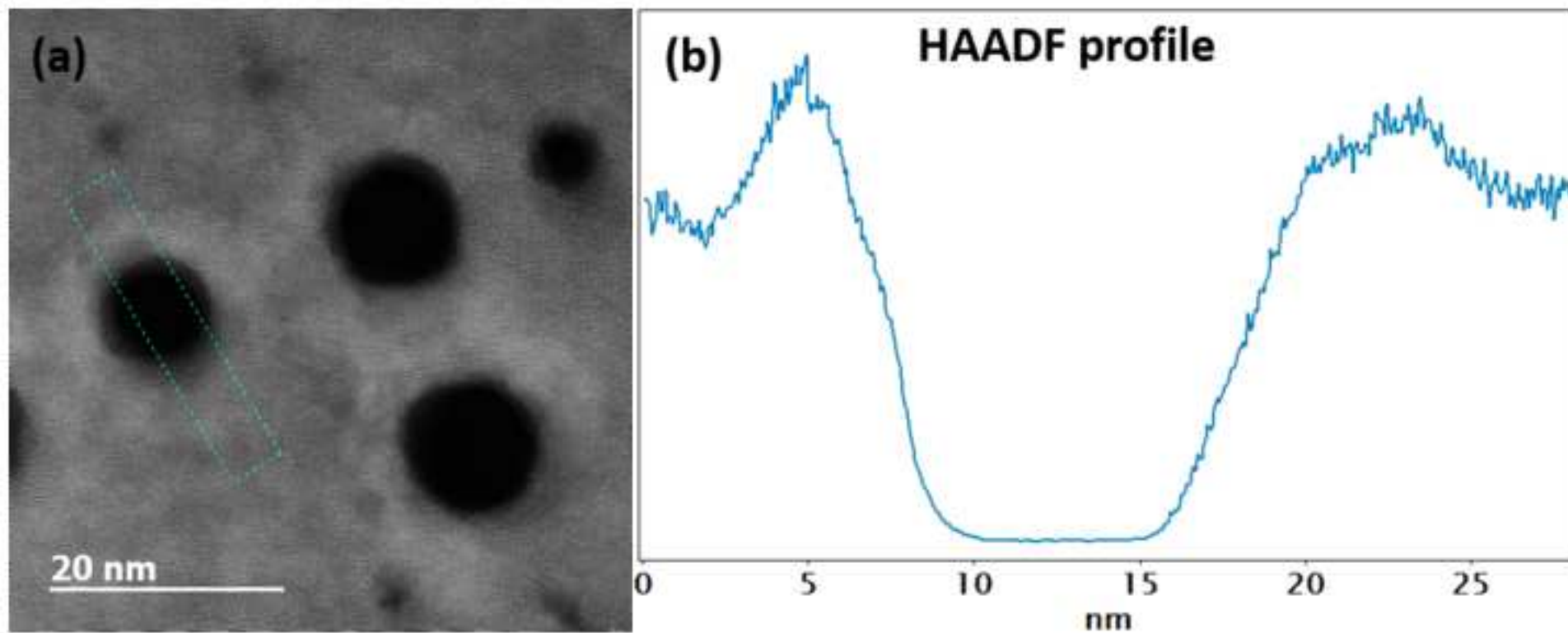
- [1] F. Ponce, D. Bour, Nitride-based semiconductors for blue and green light-emitting devices, *Nature*. 386 (1997) 351-359.
- [2] Y. Huang, X. Duan, Y. Cui, and C.M. Lieber, Gallium nitride nanowire nanodevices. *Nano Letters*, 2(2) (2002): 101-104.
- [3] S. Nakamura, S. Pearton, & Fasol, G. The blue laser diode: the complete story, *Measurement Science And Technology*. 12 (2001) 755-756.
- [4] S. Nakamura, M. Senoh, N. Iwasa, S. Nagahama, T. Yamada, T. Mukai, Superbright Green InGaN Single-Quantum-Well-Structure Light-Emitting Diodes, *Japanese Journal Of Applied Physics*. 34 (1995) L1332-L1335.
- [5] A. Khan, K. Balakrishnan, & T. Katona, Ultraviolet light-emitting diodes based on group three nitrides. *Nature photonics*, 2(2), (2008) 77.
- [6] J. Ackermann, N. Angert, R. Neumann, C. Trautmann, M. Dischner, T. Hagen, M. Sedlacek, Ion track diameters in mica studied with scanning force microscopy, *Nuclear Instruments And Methods In Physics Research Section B: Beam Interactions With Materials And Atoms*. 107 (1996) 181-184.
- [7] S. Mansouri, P. Marie, C. Dufour, G. Nouet, I. Monnet, H. Lebius, Swift heavy ions effects in III-V nitrides, *Nuclear Instruments And Methods In Physics Research Section B: Beam Interactions With Materials And Atoms*. 266 (2008) 2814-2818.
- [8] S. Kucheyev, J. Williams, C. Jagadish, J. Zou, G. Li, Damage buildup in GaN under ion bombardment, *Physical Review B*. 62 (2000) 7510-7522.
- [9] S. Kucheyev, J. Williams, C. Jagadish, J. Zou, V. Craig, G. Li, Ion-beam-induced porosity of GaN, *Applied Physics Letters*. 77 (2000) 1455-1457.
- [10] K. Lorenz, N. Barradas, E. Alves, I. Roqan, E. Nogales, R. Martin, K. P. O'Donnell, F. Gloux and P. Ruterana, Structural and optical characterization of Eu-implanted GaN, *Journal Of Physics D: Applied Physics*. 42 (2009) 165103.
- [11] F. Gloux, T. Wojtowicz, P. Ruterana, K. Lorenz, E. Alves, Transmission electron microscopy investigation of the structural damage formed in GaN by medium range energy rare earth ion implantation, *Journal Of Applied Physics*. 100 (2006) 073520.
- [12] P. Ruterana, B. Lacroix, K. Lorenz, A mechanism for damage formation in GaN during rare earth ion implantation at medium range energy and room temperature, *Journal Of Applied Physics*.
- [13] M. Ridgway, S. Everett, C. Glover, S. Kluth, P. Kluth, B. Johannessen, Z.S. Hussain, D.J. Llewellyn, G.J. Foran, G. de M. Azevedo, Atomic-scale structure of irradiated GaN compared to amorphised GaP and GaAs, *Nuclear Instruments And Methods In Physics Research Section B: Beam Interactions With Materials And Atoms*. 250 (2006) 287-290.
- [14] M. Ishimaru, Y. Zhang, W. Weber, Ion-beam-induced chemical disorder in GaN, *Journal Of Applied Physics*. 106 (2009) 053513.
- [15] S. Kucheyev, J. Williams, J. Zou, C. Jagadish, G. Li, Ion-beam-induced dissociation and bubble formation in GaN, *Applied Physics Letters*. 77 (2000) 3577-3579.
- [16] W. Jiang, Y. Zhang, W. Weber, J. Lian, R. Ewing, Direct evidence of N aggregation and diffusion in Au⁺ irradiated GaN, *Applied Physics Letters*. 89 (2006) 021903.
- [17] A. Dunlop, D. Lesueur, P. Legrand, H. Dammak, J. Dural, Effects induced by high electronic excitations in pure metals: A detailed study in iron, *Nuclear Instruments And Methods In Physics Research Section B: Beam Interactions With Materials And Atoms*. 90 (1994) 330-338.
- [18] P. Stampfli, Electronic excitation and structural stability of solids, *Nuclear Instruments And Methods In Physics Research Section B: Beam Interactions With Materials And Atoms*. 107 (1996) 138-145.
- [19] P. Stampfli, K. Bennemann, Theory for the instability of the diamond structure of Si, Ge, and C induced by a dense electron-hole plasma, *Physical Review B*. 42 (1990) 7163-7173.
- [20] M. Toulemonde, W. Assmann, C. Dufour, A. Meftah, C. Trautmann, Nanometric transformation of the matter by short and intense electronic excitation: Experimental data versus inelastic thermal spike model, *Nuclear Instruments And Methods In Physics Research Section B: Beam Interactions With Materials And Atoms*. 277 (2012) 28-39.
- [21] M. Toulemonde, E. Paumier, C. Dufour, Thermal spike model in the electronic stopping power regime, *Radiation Effects And Defects In Solids*. 126 (1993) 201-206.
- [22] F. Moisy, M. Sall, C. Grygiel, A. Ribet, E. Balanzat, I. Monnet, Optical bandgap and stress variations induced by the formation of latent tracks in GaN under swift heavy ion irradiation, *Nuclear Instruments And Methods In Physics Research Section B: Beam Interactions With Materials And Atoms*. 431 (2018) 12-18.
- [23] S. Kucheyev, H. Timmers, J. Zou, J. Williams, C. Jagadish, G. Li, Lattice damage produced in GaN by swift heavy ions, *Journal Of Applied Physics*. 95 (2004) 5360-5365.

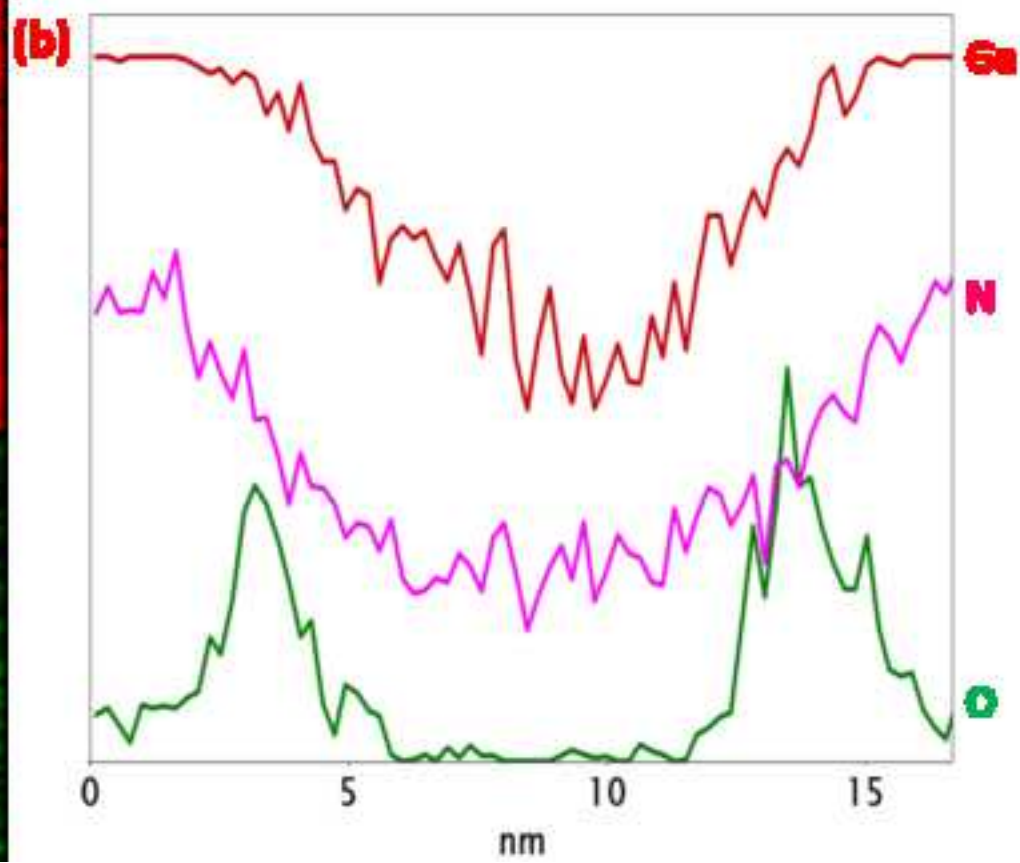
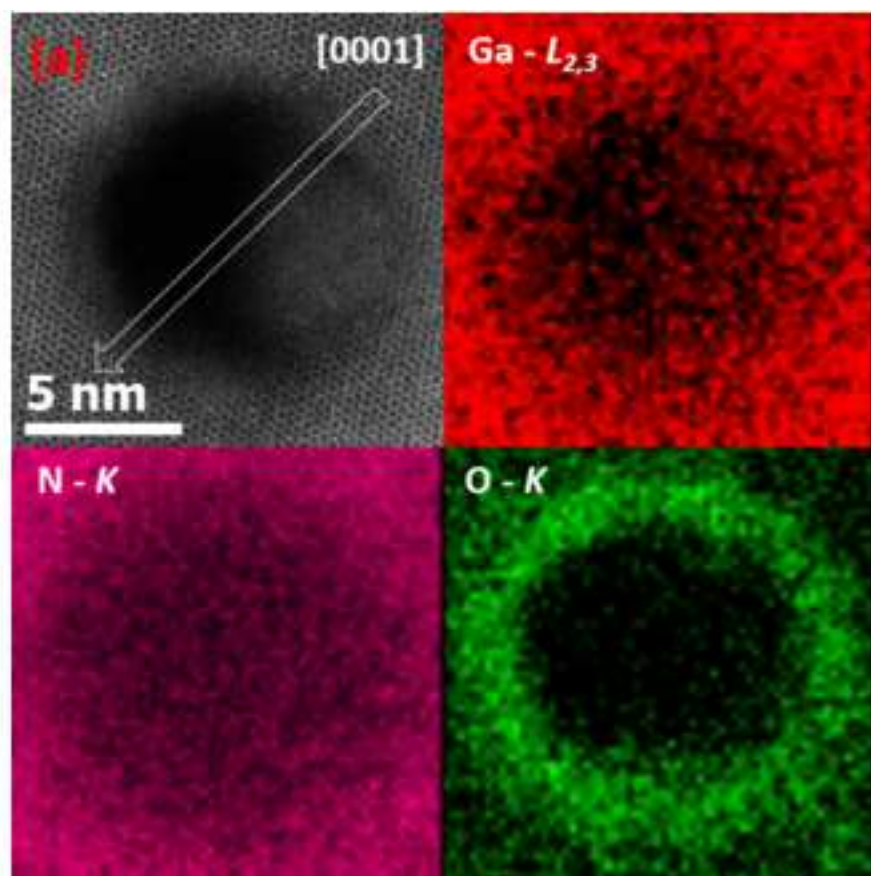
- 1 [24] F. Moisy, M. Sall, C. Grygiel, E. Balanzat, M. Boisserie, B. Lacroix, P.Simon, I.Monnet, Effects of electronic and
2 nuclear stopping power on disorder induced in GaN under swift heavy ion irradiation, Nuclear Instruments And
3 Methods In Physics Research Section B: Beam Interactions With Materials And Atoms. 381 (2016) 39-44.
- 4 [25] P. Hu, J. Liu, S. Zhang, K. Maaz, J. Zeng, H. Guo, P.F. Zhai, J.L. Duan, Y.M. Sun, M.D. Hou, Raman investigation
5 of lattice defects and stress induced in InP and GaN films by swift heavy ion irradiation, Nuclear Instruments And
6 Methods In Physics Research Section B: Beam Interactions With Materials And Atoms. 372 (2016) 29-37.
- 7 [26] S. Mansouri, P. Marie, C. Dufour, G. Nouet, I. Monnet, H. Lebius, Swift heavy ions effects in III–V nitrides, Nuclear
8 Instruments And Methods In Physics Research Section B: Beam Interactions With Materials And Atoms. 266 (2008)
9 2814-2818.
- 10 [27] M. Karlušić, R. Kozubek, H. Lebius, B. Ban-d’Etat, R. Wilhelm, M. Buljan, Z. Siketić, F. Scholz, T. Meisch, M.
11 Jakšić, Response of GaN to energetic ion irradiation: conditions for ion track formation, Journal Of Physics D:
12 Applied Physics. 48 (2015) 325304.
- 13 [28] A. Kumar, R. Singh, P. Kumar, U. Singh, K. Asokan, P. Karaseov A. I. Titov, D. Kanjilal, In-situ transport and
14 microstructural evolution in GaN Schottky diodes and epilayers exposed to swift heavy ion irradiation, Journal Of
15 Applied Physics. 123 (2018) 161539.
- 16 [29] A. Kumar, A. Hähnel, D. Kanjilal, R. Singh, Electrical and microstructural analyses of 200 MeV Ag¹⁴⁺ ion irradiated
17 Ni/GaN Schottky barrier diode, Applied Physics Letters. 101 (2012) 153508.
- 18 [30] A. Kumar, T. Kumar, A. Hähnel, D. Kanjilal, R. Singh, Dynamics of modification of Ni/n-GaN Schottky barrier
19 diodes irradiated at low temperature by 200 MeV Ag¹⁴⁺ ions, Applied Physics Letters. 104 (2014) 033507.
- 20 [31] M. Sall, I. Monnet, F. Moisy, C. Grygiel, S. Jublot-Leclerc, S. Della–Negra, M Toulemonde, E. Balanzat, Track
21 formation in III-N semiconductors irradiated by swift heavy ions and fullerene and re-evaluation of the inelastic
22 thermal spike model, Journal Of Materials Science. 50 (2015) 5214-5227.
- 23 [32] L. Marks, P. Voyles, When is Z-Contrast D-Contrast?, Microscopy Today. 22 (2014) 65-65.
- 24 [33] [11] S. Lazar, G. Botton, M. Wu, F. Tichelaar, H. Zandbergen, Materials science applications of HREELS in near
25 edge structure analysis and low-energy loss spectroscopy, Ultramicroscopy. 96 (2003) 535-546.
- 26 [34] M. Katsikini, F. Pinakidou, E. Paloura, W. Wesch, Identification of implantation-induced defects in GaN: A near-
27 edge x-ray absorption fine structure study, Applied Physics Letters. 82 (2003) 1556-1558.
- 28 [35] Y. Xin, E. James, I. Arslan, S. Sivananthan, N. Browning, S. Pennycook, F. Omnès, B. Beaumont, J-P. Faurie, P.
29 Gibart, Direct experimental observation of the local electronic structure at threading dislocations in metalorganic
30 vapor phase epitaxy grown wurtzite GaN thin films, Applied Physics Letters. 76 (2000) 466-468.
- 31 [36] B. Lacroix, V. Godinho, A. Fernández, Nitrogen Nanobubbles in a-SiO_xN_y Coatings: Evaluation of Its Physical
32 Properties and Chemical Bonding State by Spatially Resolved Electron Energy-Loss Spectroscopy, The Journal Of
33 Physical Chemistry C. 120 (2016) 5651-5658.
- 34 [37] A. Kovács, B. Schaffer, M. Moreno, J. Jinschek, A. Craven, T. Dietl, A. Bonanni, R. E. Dunin-Borkowski,
35 Characterization of Fe-N nanocrystals and nitrogen-containing inclusions in (Ga,Fe)N thin films using transmission
36 electron microscopy, Journal Of Applied Physics. 114 (2013) 033530.
- 37 [38] W. Utsumi, H. Saitoh, H. Kaneko, T. Watanuki, K. Aoki, O. Shimomura, Congruent melting of gallium nitride at 6
38 GPa and its application to single-crystal growth, Nature Materials. 2 (2003) 735-738.
- 39 [39] R. E. D. Rivas, Growth of GaN Nanowires: A Study Using In Situ Transmission Electron Microscopy (Doctoral
40 dissertation, Arizona State University). (2010)
- 41 [40] I. Bae, W. Jiang, C. Wang, W. Weber, Y. Zhang, Thermal evolution of microstructure in ion-irradiated GaN, Journal
42 Of Applied Physics. 105 (2009) 083514.
- 43 [41] W. Jiang, Y. Zhang, W. Weber, J. Lian, R. Ewing, Direct evidence of N aggregation and diffusion in Au⁺ irradiated
44 GaN, Applied Physics Letters. 89 (2006) 021903.
- 45
46
47
48
49
50
51
52
53
54
55
56
57
58
59
60
61
62
63
64
65

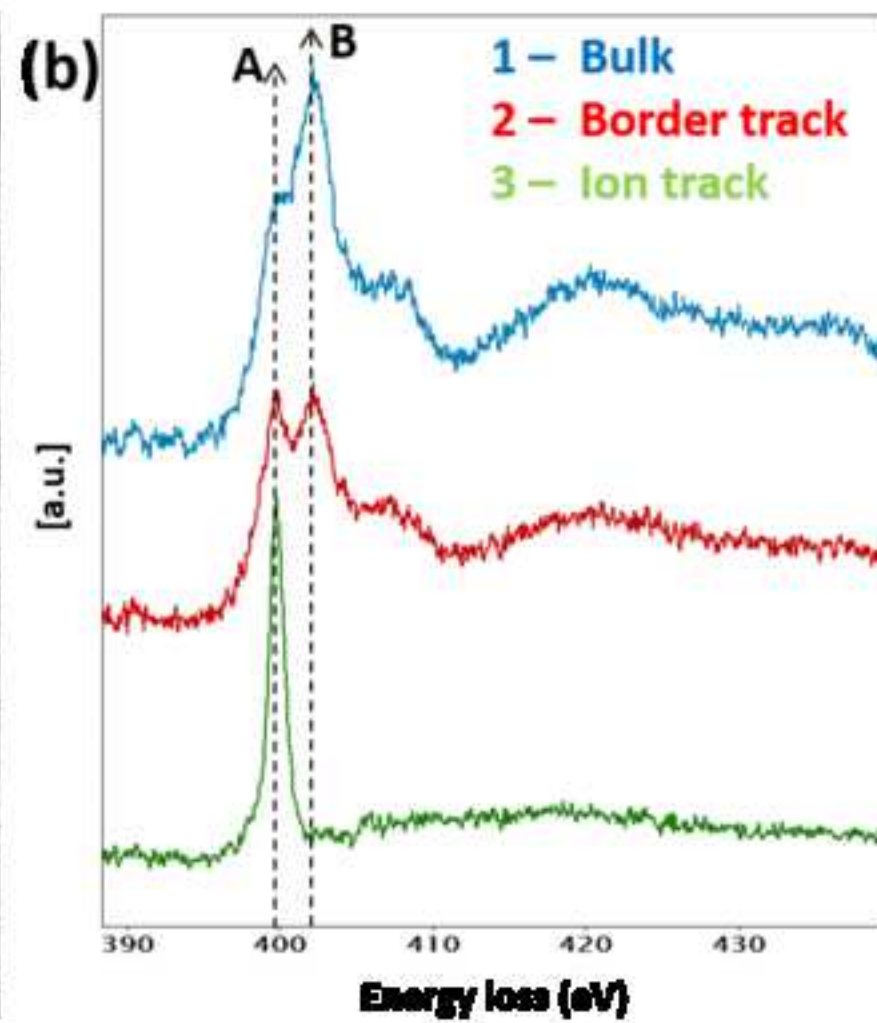
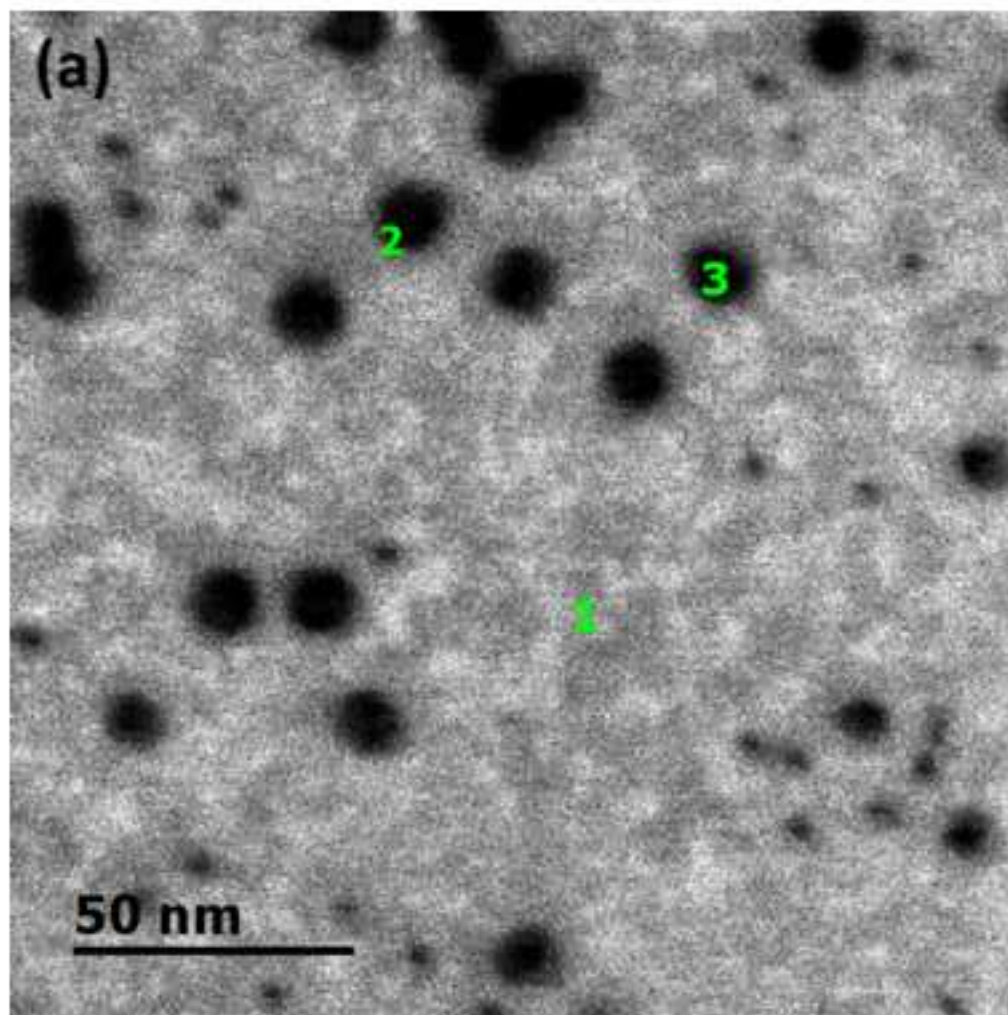


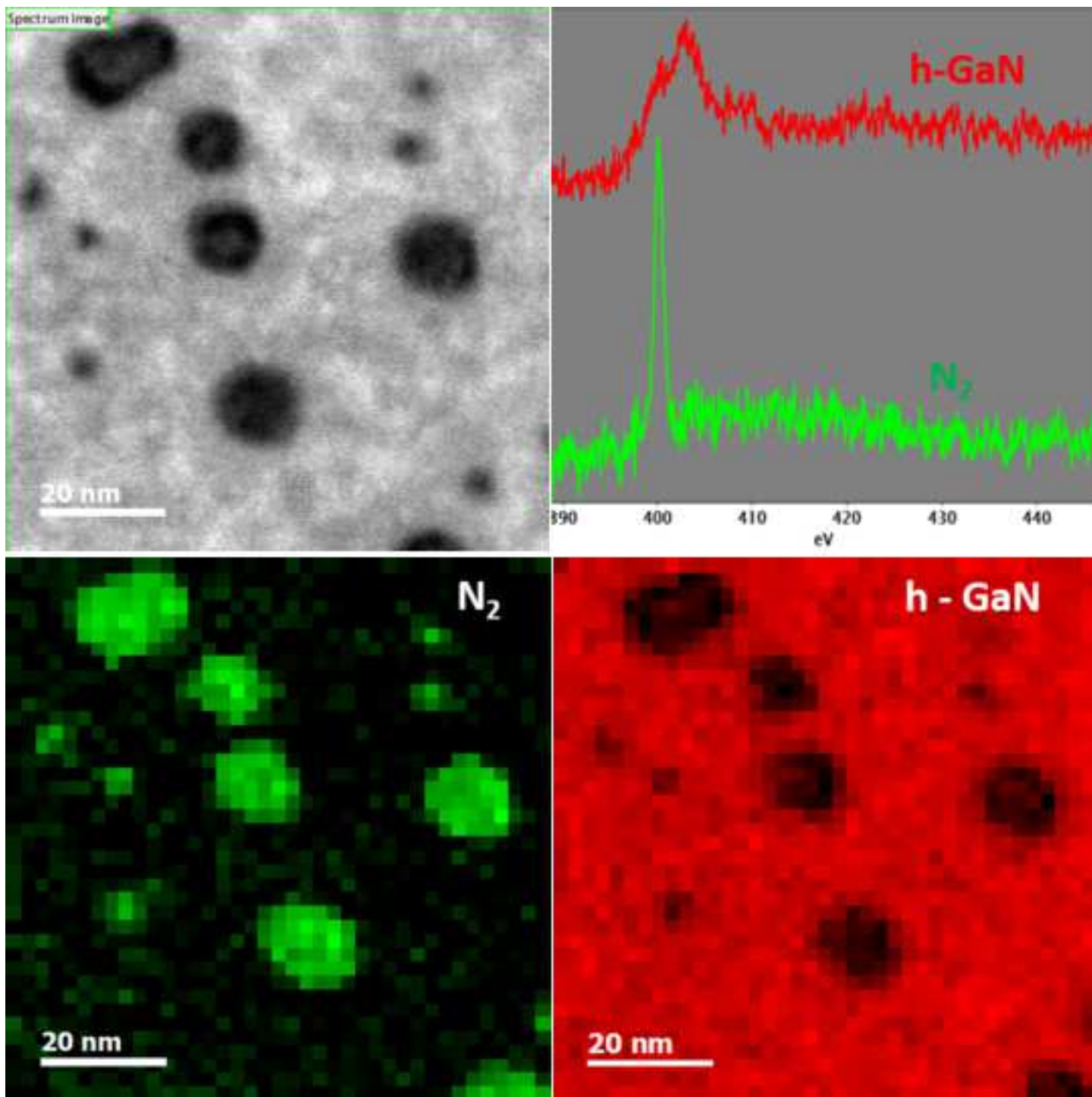












This file could not be included in the PDF because the file type is not supported.

